Ann. Acad. Rom. Sci.
Ser. Math. Appl.
ISSN 2066-6594 Vol. 17, No. 3/2025

PATTERN FORMATION AND OSCILLATORY SOLUTIONS BY NUMERICAL SIMULATIONS OF A SPACE-FRACTIONAL VEGETATION-WATER MODEL IN ARID AND SEMI-ARID ENVIRONMENTS*

Alessandra Jannelli† Maria Paola Speciale‡

Dedicated to Prof. Liliana Restuccia on the occasion of her 70th anniversary

DOI 10.56082/annalsarscimath.2025.3.227

Abstract

In this paper, we introduce a space-fractional mathematical model to describe the dynamics and interactions between vegetation and water in arid and semi-arid environments, both on flat and sloped terrains. The fractional model links two processes, such as water flows over inclined surfaces and water spreads on flat terrain, enabling the study of pattern formation with different slopes of the domain. The first process is usually described by the Klausmeier model, and the second one by the Klausmeier-Gray-Scott model, which describes water diffusion. In the proposed fractional model, the fractional Caputo derivative term allows for modeling an anomalous transport phenomenon and the non-locality of the water advection process. Oscillatory dynamics and vegetation patterns are demonstrated through numerical simulations, using a migration speed derived from a stability analysis and resulting

*Accepted for publication on October 18, 2025

†ajannelli@unime.it, Department of Mathematical and Computer Sciences, Physical Sciences and Earth Sciences, University of Messina, Viale F. Stagno d'Alcontres 31, 98166 Messina

‡mpspeciale@unime.it, Department of Mathematical and Computer Sciences, Physical Sciences and Earth Sciences, University of Messina, Viale F. Stagno d'Alcontres 31, 98166 Messina

as a function of the fractional parameter. The computational results demonstrate the robustness and effectiveness of the fractional model, which captures ecological behaviors and anomalous transport mechanisms in different terrains.

Keywords: pattern dynamics, Klausmeier and Klausmeier-Gray-Scott models, space-fractional Caputo derivative, Hopf bifurcation of the migration speed, explicit rectangular method.

MSC: 93C20, 26A33, 34C23,65C20.

1 Introduction

Vegetation patterns frequently emerge in arid and semi-arid regions [23, 28]. On sloped terrain, vegetation often organizes into banded structures aligned perpendicular to the slope direction, a phenomenon attributed to the downhill flow of water [2]. Such patterns can also form with and without slopes [3], [16]- [18], [29]. These phenomena are commonly modeled using reaction-diffusion equations with an advection term describing the water transport. In this context, one of the most widely used models is the Klausmeier (KL) model [16], a system of two coupled reaction-diffusion-advection partial differential equations modeling the dynamics of water and plant biomass. The KL model is among the earliest and simplest continuous models describing the pattern formation driven by water redistribution.

The dimensionless Klausmeier model (see [16], [7], [24]- [27]), in an one dimensional domain, is the following

$$\begin{cases} \frac{\partial u}{\partial t} = \frac{\partial^2 u}{\partial x^2} - m\,u + u^2 w, \\ \frac{\partial w}{\partial t} = \nu \frac{\partial w}{\partial x} - w - u^2 w + a. \end{cases} \tag{1}$$

This model describes the dynamics and the interaction between plant biomass $u(t,x)$ and water $w(t,x)$ in arid and semi-arid ecosystems. a, m, and ν are positive constants and represent rainfall input, plant mortality (i.e., vegetation death rate), and the slope gradient in dimensionless form, respectively. The linear term$-m\,u$ accounts for plant mortality, while the nonlinear term $u^2 w$ represents water uptake by plants. This uptake also drives plant growth, as water absorbed by vegetation is converted into biomass at a constant rate: this is reflected by the same nonlinear term appearing in both equations of the model. Finally, the loss of water due to evaporation by at a rate normalized is described by $-w$. The system is considered on a one-dimensional domain with a constant, generally gentle slope, where increasing x corresponds to the uphill direction. The parameters a, m, and ν are chosen to

reflect different ecological conditions. Specifically, the slope parameter ν is assumed to be large (i.e., $\nu \gg 1$) to model downhill water advection, while a and m vary within the ranges $[0.1, 3.0]$ and $[0.05, 2.0]$, respectively [16,22].

We now consider a modified version of the Klausmeier model in which the water advection term is replaced by a diffusion term, representing plant growth on flat terrain rather than sloped land. The resulting dimensionless model, also known as the diffusion Klausmeier–Gray–Scott model (KL–GS), is given by

$$\begin{cases} \frac{\partial u}{\partial t} = \frac{\partial^2 u}{\partial x^2} - m\,u + u^2 w, \\ \frac{\partial w}{\partial t} = \nu \frac{\partial^2 w}{\partial x^2} - w - u^2 w + a. \end{cases} \tag{2}$$

This system, generally applied in chemistry to describe the interaction between two concentrations of reacting substances, substrate and activator [8], in this context, models the dynamics and interaction between water and plants in a flat, diffusing water domain. All terms and coefficients have the same physical meaning as those in the KL model, except that the advection term $\nu \frac{\partial w}{\partial x}$ is replaced by the diffusion term $\nu \frac{\partial^2 w}{\partial x^2}$, so ν is a diffusion coefficient. In the Klausmeier model (1), the parameter ν reflects the relative downstream water flows and plant dispersal. In the model (2), because plants grow on flat rather than hilly terrain, the diffusion effect occurs rather than the advection effect.

The spatial non-locality arises from the strong variability and long-range dependence associated with terrain slope. Due to their inherent non-local nature, fractional derivatives provide a more appropriate framework for modeling such phenomena than classical integer-order derivatives. It has been shown that mathematical models describing diffusion in complex systems are quite efficient when fractional operators are used and usually the models are fractional advection-reaction-diffusion models as in [9]- [15], [19].

In this paper, a new fractional mathematical model is proposed to describe the dynamics and interactions between vegetation and water in both flat and non-flat domains. Using the spatial fractional Caputo operator, the model accounts for the anomalous physical processes that lead to vegetation patterns

$$\begin{cases} \frac{\partial u}{\partial t} = \frac{\partial^2 u}{\partial x^2} - m\,u + u^2 w, \\ \frac{\partial w}{\partial t} = \nu \partial_x^{\alpha+1} w - w - u^2 w + a, \end{cases} \tag{3}$$

where $\partial_x^{\alpha+1}$ is the fractional Caputo operator defined as follows [5,20]

$$\partial_x^{\alpha+1} w(x,t) = \partial_x^{\alpha} \left(\partial_x w(x,t)\right) = \tag{4}$$

$$= \frac{1}{\Gamma(1-\alpha)} \int_0^x \frac{\partial^2 w(s,t)}{\partial s^2} (x-s)^{-\alpha} ds, \quad 0 < \alpha < 1,$$

with $\Gamma(\cdot)$ the Euler's gamma function and α fractional derivative order. In the context of Caputo's fractional derivative, when $\alpha = 0$, according to the definition, a first-order derivative is obtained, and setting $\partial_x w(0,t) = 0$, the model (3) reduces to the classical KL model (1), which describes advection-dominated dynamics. Conversely, for $\alpha = 1$, the fractional derivative becomes a second-order derivative, restoring the KL-GS model (2), which describes classical diffusion.

Our focus is on the intermediate regime $0 < \alpha < 1$. Thus, the proposed fractional model provides a transition from the KL model to the KL-GS model through the variation of the parameter α. The purpose of this paper is to demonstrate how the proposed fractional model can capture the behavior of the solution by varying the fractional parameter α associated with the domain slope, preserving the vegetation pattern formation. We find that the patterns have a migration speed in the uphill direction that is determined through an analytical stability analysis of the Hopf bifurcation, and the study is further supported by numerical simulations.

In the present study, we introduce the fractional Caputo operator directly into the partial differential model, proposing a new fractional model given in terms of the fractional partial differential equations and then introducing the traveling wave solutions. In contrast, in our recent paper [15], we defined a new fractional model, given by fractional ordinary differential equations, obtained after applying the traveling wave solutions.

The paper plan is as follows. In Section 2, we reduce the new fractional model to fractional ordinary differential equations by considering the traveling wave solution and the stability analysis of the reduced model is studied. In Section 3, we perform the stability analysis of the equilibrium points and we find the values of the migration speed at which the Hopf bifurcation occurs and the pattern formation is guaranteed. In Section 4, we present the numerical method to solve the new fractional model, proving the pattern formation for various values of the fractional parameter. The obtained numerical solutions validate the analytical results and confirm the reliability and effectiveness of the proposed model. The last Section is devoted to conclusions and future works.

2 Traveling wave solution and stability analysis

In this Section, we reduce the new fractional mathematical model into a system of fractional ordinary differential equations by introducing the traveling wave solution. By following a procedure applied in [15, 27], we study the stability of the new proposed fractional model (3).

2.1 Traveling wave solution and fractional ordinary differential equations

The model (3) admits the traveling wave solution

$$u(x,t) = U(x - c_\alpha t) = U(z) \qquad w(x,t) = W(x - c_\alpha t) = W(z), \tag{5}$$

where $c_\alpha > 0$ is the migration speed in the uphill direction. In terms of new variables, the model is rewritten into the fractional ordinary differential equations

$$\begin{cases} U'' + c_\alpha U' - mU + U^2 W = 0 \\ \nu\, {}_{z_0}D_z^{\alpha+1} W + c_\alpha W' - W - U^2 W + a = 0 \end{cases} \tag{6}$$

being the fractional Caputo operator ${}_{z_0}D_z^{\alpha+1}$, see [5, 20] given by

$$\begin{aligned} {}_{z_0}D_z^{\alpha+1} W(z) &= {}_{z_0}D_z^{\alpha} W'(z) \\ &= \frac{1}{\Gamma(1-\alpha)} \int_{z_0}^{z} W''(\xi)(z-\xi)^{-\alpha} d\xi, \quad 0 < \alpha < 1, \end{aligned} \tag{7}$$

where $z_0 = -c_\alpha \tau$, obtained by using the transformation $z = x - c_\alpha t$ in the Caputo operator (4). Here, τ is a fixed real number that we set equal to the final time in the numerical applications.

The model (6) admits the following three uniform steady states whose behavior depends upon the values of the parameters

$$(U_0, W_0) = (0, a), \quad (U_\pm, W_\pm) = \left(\frac{a \pm \sqrt{a^2 - 4m^2}}{2m}, \frac{a \mp \sqrt{a^2 - 4m^2}}{2} \right), \tag{8}$$

when $a > 2m$ with $m < 2$. These points are the same equilibrium points admitted by KL and KL-GS models, and we have that (U_0, W_0) is a stable one and leads to desertification, (U_-, W_-) is a saddle point, whereas the point (U_+, W_+) depends on the involved parameters [6, 27]. The Turing-type patterns and, consequently, the existence of oscillatory solutions arise for homogeneous perturbations of the point (U_+, W_+).

The main feature of the proposed formulation, model (6), lies in the assumption that the fractional operator's order α is linked to the slope of the domain. This allows the fractional model to capture uphill migration dynamics across domains with arbitrary slopes. This assumption is supported by an analytical investigation of the Hopf bifurcation associated with the migration speed. Our analysis demonstrates that the migration speed c_α, characterizing the propagation of solutions, depends on the fractional parameter α. In particular, as the slope approaches zero, α approaches the limiting value 0, for which c_α tends to 0, in agreement with observed physical behavior.

2.2 Approximation of FODEs by ODEs

Here, we perform the stability analysis of the reformulated model (6), and to this aim, we approximate the FODEs (6) to new ODEs.

To study the stability of equilibrium points, we apply the same procedure used in [15], according to an approach developed by Sheratt in [27]. By the rescaling of coordinate, $\zeta = z/\nu$, $U = \bar{U}(\zeta)$ and $W = \bar{W}(\zeta)$, the fractional model (6) is mapped into the following one

$$\begin{cases} \frac{\bar{U}''}{\nu^2} + \frac{c_\alpha}{\nu}\bar{U}' - m\bar{U} + \bar{U}^2\bar{W} = 0 \\ \frac{1}{\nu^\alpha}\,{}_{\zeta_0}D_\zeta^{\alpha+1}\bar{W} + \frac{c_\alpha}{\nu}\bar{W}' - \bar{W} - \bar{U}^2\bar{W} + a = 0. \end{cases}$$

By adding and subtracting the term $(1-\alpha)\bar{W}'$ in the second equation, we obtain

$$\begin{cases} \frac{\bar{U}''}{\nu^2} + \frac{c_\alpha}{\nu}\bar{U}' - m\bar{U} + \bar{U}^2\bar{W} = 0 \\ \frac{1}{\nu^\alpha}\,{}_{\zeta_0}D_\zeta^{\alpha+1}\bar{W} - (1-\alpha)\bar{W}' + (1-\alpha+\frac{c_\alpha}{\nu})\bar{W}' - \bar{W} - \bar{U}^2\bar{W} + a = 0, \end{cases} \tag{9}$$

where

$$\frac{1}{\nu^\alpha}\,{}_{\zeta_0}D_\zeta^{\alpha+1}\bar{W} - (1-\alpha)\bar{W}' = \begin{cases} 0 & \alpha = 0 \\ \frac{1}{\nu}\,{}_{\zeta_0}D_\zeta''\bar{W} & \alpha = 1 \end{cases}$$

with $\bar{W}'(\zeta_0) = 0$, and

$$\left| \frac{1}{\nu^\alpha}\,{}_{\zeta_0}D_\zeta^{\alpha+1}\bar{W} - (1-\alpha)\bar{W}' \right| \ll 1$$

for large values of ν and different values of α, with $0 < \alpha < 1$. Therefore, we set

$$\left| \frac{1}{\nu^{\alpha}} \, {}_{\zeta_0}D_{\zeta}^{\alpha+1} \bar{W} - (1-\alpha)\bar{W}' \right| \approx 0, \tag{10}$$

according to the analytical and numerical results obtained in [15].

Moreover, the term involving $\frac{1}{\nu^2}$, in the first equation, is negligible due to large values of ν and the order of magnitude of c_α is the same as of ν (see Sherratt [27]). so that we can study the stability and the Hopf bifurcation of the proposed system as a first-order one. By applying the following transformation to the system (9)

$$\tilde{\bar{U}} = \bar{U}, \quad \tilde{\bar{W}} = \left(1 - \alpha + \frac{\nu}{c_\alpha}\right) \bar{W}, \quad \tilde{\bar{\zeta}} = \left(1 - \alpha + \frac{c_\alpha}{\nu}\right)^{-1} \zeta, \tag{11}$$

and taking into account the assumption (10), we get

$$\begin{cases} \tilde{\bar{U}}' - M_\alpha \tilde{\bar{U}} + \tilde{\bar{U}}^2 \tilde{\bar{W}} = 0 \\ \tilde{\bar{W}}' - \tilde{\bar{W}} - \tilde{\bar{U}}^2 \tilde{\bar{W}} + A_\alpha = 0, \end{cases} \tag{12}$$

with

$$M_\alpha = \left(1 + \frac{(1-\alpha)\nu}{c_\alpha}\right) m, \qquad A_\alpha = \left(1 + \frac{(1-\alpha)\nu}{c_\alpha}\right) a.$$

2.3 Hopf bifurcation for migration speed

We study the equilibrium states of the system (12) and perform an analysis of the stability of the equilibrium points with the aim of obtaining the Hopf bifurcation for migration speed.

The equilibrium points are $(\tilde{\bar{U}}_0, \tilde{\bar{W}}_0) = (0, A_\alpha)$ and

$$(\tilde{\bar{U}}_\pm, \tilde{\bar{W}}_\pm) = \left(\frac{A_\alpha \pm \sqrt{A_\alpha^2 - 4M_\alpha^2}}{2M_\alpha}, \frac{A_\alpha \mp \sqrt{A_\alpha^2 - 4M_\alpha^2}}{2} \right),$$

for $\alpha = 0$ and $\alpha = 1$ it holds

$$(\tilde{\bar{U}}_0, \tilde{\bar{W}}_0) = (U_0, W_0), \qquad (\tilde{\bar{U}}_\pm, \tilde{\bar{W}}_\pm) = (U_\pm, W_\pm).$$

The characteristic polynomial is given by

$$\lambda^2 + (M_\alpha - 1 - \tilde{\bar{U}}_\pm^2)\lambda + M_\alpha(\tilde{\bar{U}}_\pm^2 - 1) = 0. \tag{13}$$

In this context, we are interested in finding the Hopf bifurcation point for the unstable state $(\tilde{\tilde{U}}_+, \tilde{\tilde{W}}_+)$. We obtain the Hopf bifurcation by requiring the following equality condition

$$|\arg(\lambda_{1,2})| = \left|\arctan\left(\frac{\sqrt{4M_\alpha(\tilde{\tilde{U}}_+^2 - 1) - (M_\alpha - 1 - \tilde{\tilde{U}}_+^2)^2}}{-M_\alpha + 1 + \tilde{\tilde{U}}_+^2}\right)\right| = \frac{\pi(1-\alpha)}{2}$$

with the conditions

$$M_\alpha - 1 - \tilde{\tilde{U}}_+^2 \leq 0, \quad \Delta = (M_\alpha - 1 - \tilde{\tilde{U}}_+^2)^2 - 4M_\alpha(\tilde{\tilde{U}}_+^2 - 1) < 0, \tag{14}$$

as it was proved in [15]. We get the Hopf bifurcation migration speed, c_α^{HB} for the state $(\tilde{\tilde{U}}_+, \tilde{\tilde{W}}_+)$

$$\begin{aligned} c_\alpha^{HB} = & \frac{(1-\alpha)m\,\nu}{(1-m+\tilde{\tilde{U}}_+^2)^2 + 2m\left(\tilde{\tilde{U}}_+^2 - 1\right)(\cos(\pi\alpha) - 1)} \\ & \left(1 - m + \tilde{\tilde{U}}_+^2 + (\cos(\pi\alpha) - 1)(1 - \tilde{\tilde{U}}_+^2) + \right. \\ & \left. -\sqrt{\left(\tilde{\tilde{U}}_+^2 - 1\right)\left(2\tilde{\tilde{U}}_+^2(1 - \cos(\pi\alpha))^2 + (\tilde{\tilde{U}}_+^2 + 1)\sin^2(\pi\alpha)\right)}\right), \end{aligned} \tag{15}$$

depending on the fractional parameter α and the parameters of the model a, m and ν. We observe that for $\alpha = 0$, the migration speed reduces to the classical Hopf bifurcation value $c^{HB} = \frac{m\,\nu}{1-m+U_+^2}$ of the KL model (see [27]). In contrast, as $\alpha \to 1$, the migration speed tends toward zero ($c_\alpha \to 0$). In the next Section, we prove that from the critical migration speed c_α^{HB}, a branch of the vegetation pattern emerges, which will be validated through numerical simulations.

3 Numerical method and results

The main objective of this study is to demonstrate that the proposed fractional model (6), as the parameter α varies, is in agrement with the dynamics of the classical models (1) and (2), and captures the formation of banded vegetation patterns in both sloped and flat environments. In this section, we describe the numerical method employed to solve the fractional model (6). Numerical simulations are performed for various values of the fractional parameter α, validating the effectiveness and reliability of the proposed model. We apply a one-step explicit numerical method derived from product integral

rules, which involves approximating the integral formulation of the governing equations. All simulations are performed using MATLAB on an Intel Core i7 processor. We use a large number of nodes to obtain highly accurate solutions and then, in order to keep the computational cost not too high.

We rewrite the system (6) in the following form

$$\begin{cases} U'' = -c_\alpha U' + mU - U^2 W, \\ {}_{z_0}D_z^{\alpha+1} W = \dfrac{1}{\nu}\left(-c_\alpha W' + W + U^2 W - a\right), \end{cases}$$

completed with suitable initial conditions. As usual, we introduce the following assignments

$${}^1u(z) = U(z), \qquad {}^2u(z) = W(z), \qquad {}^3u(z) = U'(z), \qquad {}^4u(z) = W'(z),$$

such that we obtain the system

$$\begin{cases} {}^1u' = {}^3u \\ {}^2u' = {}^4u \\ {}^3u' = -c_\alpha^3 u + m\ {}^1u - \ ({}^1u)^2\ {}^2u \\ {}_{z_0}D_z^\alpha\ {}^4u = \dfrac{1}{\nu}\left(-c_\alpha\ {}^4u + \ {}^2u + \ ({}^1u)^2\ {}^2u - a\right). \end{cases} \tag{16}$$

For solving the fractional model (16), we set a integration step-size Δz and define a uniform computational grid of $J+1$ grid-points, namely z_j, with $z_j = z_0 + j\Delta z$, for $j = 0, \cdots, J$. Then, at each of the grid-points z_j, we define ${}^iu_j$ for $j = 1, \ldots, 4$. In particular, $U_j = {}^1u_j \approx U(z_j)$ and $W_j = {}^2u_j \approx W(z_j)$ are the numerical approximations of the exact solutions, the density of plant and water, respectively.

Starting from the fourth equation of the above system, we introduce its equivalent Volterra integral formulation

$${}^4u(z) = \ {}^4u_0 + \frac{1}{\Gamma(\alpha)} \int_{z_0}^{z} f(s,\ {}^4u(s))(z-s)^{\alpha-1} ds, \tag{17}$$

where

$$f(z,\ {}^4u(z)) = \frac{1}{\nu}\left(-c_\alpha\ {}^4u + \ {}^2u + \ ({}^1u)^2\ {}^2u - a\right).$$

For the problem under study, the equivalent Volterra integral equation at $z = z_{j+1}$ reduces to

$$\begin{aligned} {}^4u(z_{j+1}) &= {}^4u_0 + \frac{1}{\Gamma(\alpha)} \int_{z_0}^{z_{j+1}} f(s,\ {}^4u(s))(z_{j+1}-s)^{\alpha-1} ds \\ &= {}^4u_0 + \frac{1}{\Gamma(\alpha)} \sum_{k=0}^{j} \int_{z_k}^{z_{k+1}} f(s,\ {}^4u(s))(z_{j+1}-s)^{\alpha-1} ds. \end{aligned} \tag{18}$$

Now, in each sub-interval $[z_k, z_{k+1}]$ we can substitute $f(z, {}^4u(z))$ with an interpolation polynomial, so that the resulting integrals can be exactly evaluated. In order to compute ${}^4u(z_{j+1})$, to approximate the integral on the right-hand side of the (18), we use the rectangular explicit rule, obtaining the following explicit formula

$$ {}^4u_{j+1} = {}^4u_0 + \frac{1}{\Gamma(\alpha)} \sum_{k=0}^{j} a_k f(z_k, {}^4u_k) \qquad j = 0, \cdots, J-1 \tag{19} $$

with

$$ a_k = \int_{z_k}^{z_{k+1}} (z_{j+1} - s)^{\alpha-1} ds = \frac{1}{\alpha} \left[(z_{j+1} - z_k)^\alpha - (z_{j+1} - z_{k+1})^\alpha \right] . $$

Finally, operating in the same way for the first three equations, we obtain the following explicit method with an order of accuracy equal to one

$$ \begin{cases} {}^1u_{j+1} = {}^1u_j + \Delta z \, {}^3u_j \\ {}^2u_{j+1} = {}^2u_j + \Delta z \, {}^4u_j \\ {}^3u_{j+1} = {}^3u_j + \Delta z \left(-c_\alpha \, {}^3u_j + m \, {}^1u_j - ({}^1u_j)^2 \, {}^2u_j \right) \\ {}^4u_{j+1} = {}^4u_0 + \dfrac{1}{\nu \, \Gamma(\alpha)} \displaystyle\sum_{k=0}^{j} a_k \left(-c_\alpha \, {}^4u_k + {}^2u_k + ({}^1u_k)^2 \, {}^2u_k - a \right) . \end{cases} \tag{20} $$

In the following, we solve the system (6), assigned the parameters a, m and ν, with initial conditions:

$$ {}^1u_0 = U_0, \qquad {}^2u_0 = \frac{m}{U_0}, \qquad {}^3u_0 = 0, \qquad {}^4u_0 = 0 $$

on computational domain $[z_0, z_{\max}] = [-c_\alpha \tau, 500]$ with $\tau = 10$. We set $\Delta z = 0.06$ such that $J = \left\lceil \frac{z_{\max} - z_0}{\Delta z} \right\rceil$. The initial conditions ${}^1u_0$ and ${}^2u_0$ are chosen as perturbations of the equilibrium point (U_+, W_+), obtained by (8). Moreover, the migration speed c_α is set such that $c_\alpha < c_\alpha^{HB}$ to obtain oscillatory solutions.

3.1 A numerical application

To validate the theoretical results, we present an application of interest concerning the vegetation pattern formation obtained by numerically solving the proposed fractional model. By the numerical solutions, we show that vegetation pattern formation arises when the migration speed c_α assumes smaller

values than the migration speed c_α^{HB}, according to the theory performed by Sherratt [27] for the KL model.

We set the parameters involved in the models as follows

$$a = 1.4, \quad m = 0.45, \qquad \nu = 182.5,$$

so we get of $(U_+, W_+) = (2.74709, 0.364021)$ and as perturbation $({}^1u_0, {}^2u_0)$ $= (2.52732, 0.17805)$. Varying α in the range $]0, 1[$, we obtain the profile of migration speed c_α^{HB} given by (15). When $\alpha = 0$, we have $c_\alpha^{HB} = c^{HB} = 10.1433$ and when $\alpha = 1$, $c_\alpha = 0$, see [15, 27] .

For solving the fractional model, we find the value c_α, reported in Tab. 1, for each parameter value α to get oscillatory solutions and pattern formation, such that $c_\alpha < c_\alpha^{HB}$.

α	0.0	0.1	0.2	0.3	0.4	0.5	0.6	0.7	0.8	0.9	$\to 1$
c_α	10.05	6.475	4.344	2.982	2.070	1.436	0.972	0.627	0.363	0.156	$\to 0$

Table 1: Values of c_α depending on the fractional parameter α.

The values (α, c_α), reported in Table 1, are used as interpolation nodes to build the interpolation cubic spline $p(\alpha)$ and then to obtain the values of c_α, $\forall\alpha$ with $0 < \alpha < 1$. In Fig. 1, we show the migration speeds c_α (blue points), c_α^{HB} (green line) and $p(\alpha)$ obtained by the interpolation with the cubic spline (black line).

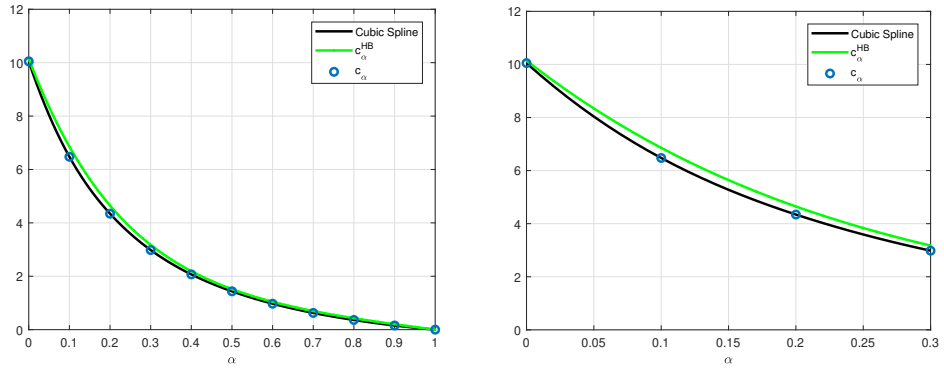

Figure 1: Migration speed c_α^{HB}, depending on α, given by (15) for $\nu = 182.5$. Right frame: zoom of the left frame.

In Figs. 2 and 3, we report the numerical solutions U_j and W_j of the fractional model (6) obtained for different values of α, with $0 < \alpha < 1$ and with the corresponding migration speed c_α reported in Tab.1.

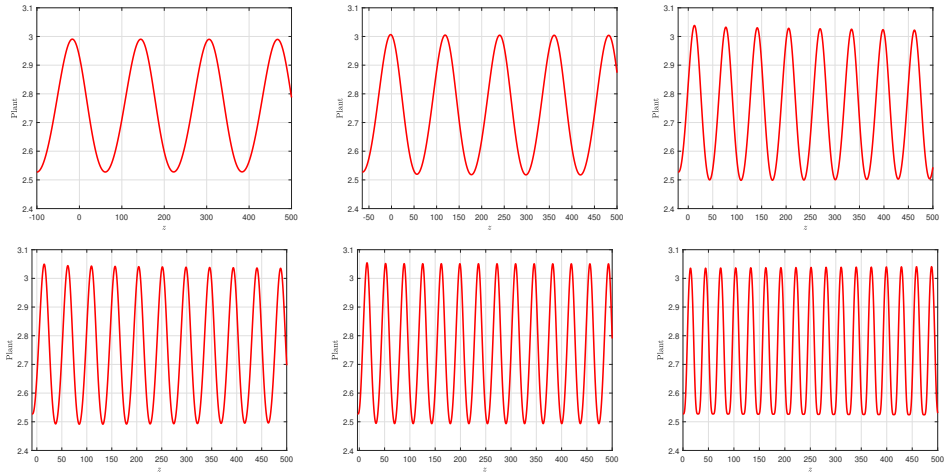

Figure 2: Numerical solutions U_j of the concentration of the plant $U(z_j)$ of the KL and KL-GS models and for different values of $0 < \alpha < 1$; from left to right: KL model, $\alpha = 0.1$, $\alpha = 0.4$, $\alpha = 0.6$, $\alpha = 0.8$ and KL-GS model.

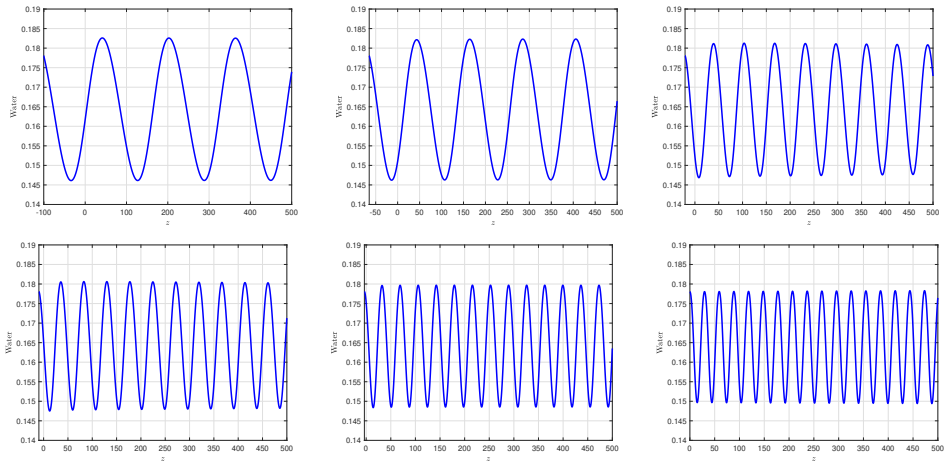

Figure 3: Numerical solutions W_j of the concentration of the water $W(z_j)$ of the KL and KL-GS models and for different values of $0 < \alpha < 1$; from left to right: KL model, $\alpha = 0.1$, $\alpha = 0.4$, $\alpha = 0.6$, $\alpha = 0.8$ and KL-GS model.

Figs. 4 and 5 display the numerical solutions of $u(t,x)$ and $w(t,x)$, computed for various values of α, at the final time $t = 10$. The solutions are evaluated in the reference domain taking into account that $z = x - c_\alpha t$, where c_α denotes the migration speed dependent on α. Cubic spline interpolation is employed to reconstruct the solutions across the entire computational domain. The numerical results illustrate the migration of vegetation patterns in the uphill direction and reveal how their trajectories vary with α, so that we can affirm that the fractional order parameter is linked to the slope of the terrain. This variation in α leads to different values of the migration speed c_α, resulting in distinct uphill movement behaviors. On slopes, the vegetation forms alternating bands of plant cover and bare ground, aligned parallel to the level curves. The space-time plots in Figures 4 and 5 clearly show the evolution of both vegetation and water distributions. These plots highlight the anomalous transport phenomena, with the direction of pattern migration consistently oriented towards increasing x. For each α, the patterns propagate at a constant speed in this positive direction, confirming the uphill migration of vegetation.

The fractional formulation of the model captures the oscillatory nature of the solutions, which is essential for reproducing vegetation pattern formation and migration in arid and semi-arid regions with arbitrary slopes.

We observe that when $\alpha = 0$ the new system models the classical advection process that describes the downward-oriented flow of the water and, for $\alpha = 1$, it models the classical diffusion process where the water diffuses, there is not advection term and the water does not flow. As α approaches 0, the solutions tend toward those of the KL model, where advection dominates. In the limit $\alpha \to 1$, advection becomes negligible, and the solutions closely resemble those of the KL–GS model, characterized by classical diffusion. In the fractional model, as the α parameter increases, from zero to one, the trajectory of the solution changes due to the decrease of the migration speed related to the decreasing of the slope of the domain that tends to become flat, The differences in the trajectories of the vegetation patterns depend on the value of the migration speed c_α, a function of the fractional parameter α that is linked to the slope of the domain.

Remark. Furthermore, another important result of the present study is to find the values of c_α for all α by using the cubic spline interpolation reconstruction $p(\alpha)$, based on the data presented in Table 1, that allows to compute numerical solutions for any value of α in the interval $0 < \alpha < 1$, as demonstrated in [15].

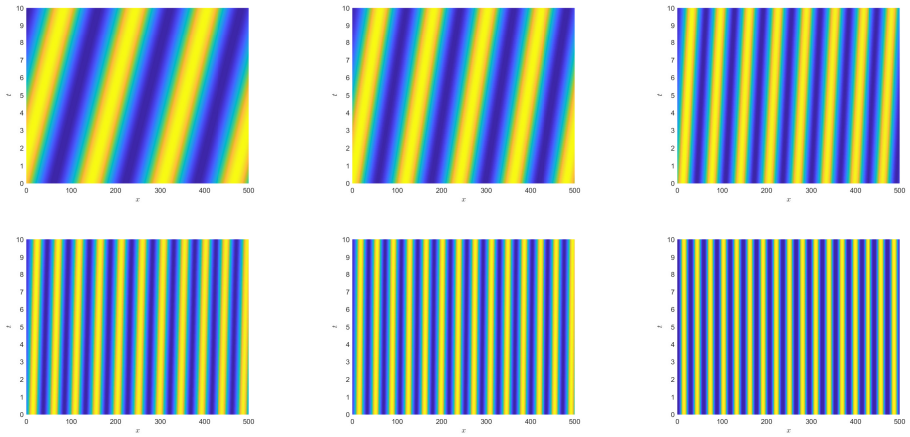

Figure 4: Numerical solutions of the concentration of plants $u(t, x)$ at final time $t = 10$. From left to right: KL model, FM with $\alpha = 0.1$, $\alpha = 0.4$, $\alpha = 0.6$, $\alpha = 0.8$ and KL-GS model.

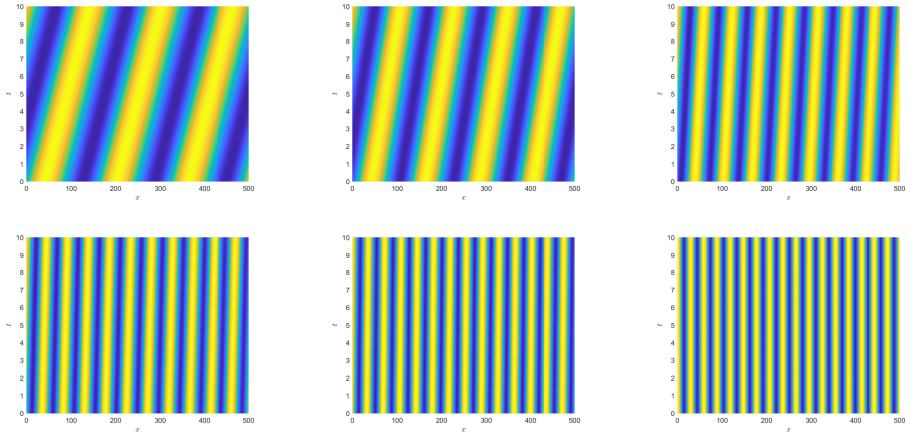

Figure 5: Numerical solutions of the concentration of water $w(t, x)$ at final time $t = 10$. From left to right: KL model, FM with $\alpha = 0.1$, $\alpha = 0.4$, $\alpha = 0.6$, $\alpha = 0.8$ and KL-GS model.

4 Conclusions

In this paper, we develop a novel fractional model to describe the dynamics and the interaction between vegetation and water concentration in non-flat, low-lying arid and semi-arid regions. The key idea behind the proposed

formulation is to link the order of the fractional operator to the slope of the domain. This approach allows the model to capture how vegetation migration changes with varying terrain inclinations and different values of the fractional parameter α. The proposed fractional framework establishes a connection between the classical KL model and the KL–GS model, with the transition governed by the parameter α. This modeling assumption is supported by an analytical investigation of the Hopf bifurcation of the migration speed, denoted by c_α^{HB}, demonstrating that it is a function of α. Consequently, we prove that the migration speed c_α depends on α. This point marks the onset of pattern formation, where vegetation stripes begin to emerge. The fractional formulation enables the system to exhibit oscillatory behavior in the solutions, thus ensuring the formation of vegetation patterns in arid and semi-arid regions, regardless of slope. Numerical simulations confirm the self-organization of vegetation into migrating bands, where the migration speed c_α satisfies $c_\alpha < c_\alpha^{HB}$, and is influenced by the terrain's slope. The numerical findings are in strong agreement with the theoretical predictions.

The analytical and numerical study of a new fractional model with a variable rainfall rate will represent the future direction of the research. Moreover, other numerical methods, as, for example, the methods implemented in [1,4], could be used to confirm results obtained in the present study.

Acknowledgements. A.J. and M.P.S are members of the GNCS-INdAM Research Group and of the GNFM-INdAM Research Group, respectively.

This research is supported by the project: "Strategie HPC e modelli fisico-matematici per la previsione di eventi meteorologici estremi (HPC-XTREME)". CUP B83C22002830001 - codice identificativo CN00000013. Bando PRIN 2022 PNRR - D.D. n. 341 del 15/03/2022.

References

[1] A. Aimi, L. Desiderio, Diligenti and C.A. Guardasoni, Numerical study of energetic bem-fem applied to wave propagation in 2D multidomains, *Publ. Inst. Math.* 96 (2014), 5–22.

[2] F. Borgogno, P. D'Odorico, F. Laio and L. Ridolfi, Mathematical models of vegetation pattern formation in ecohydrology, *Rev. Geophys.* 47 (2009), 2007RG000256.

[3] V. Deblauwe, N. Barbier, P. Couteron, O. Lejeune and J. Bogaert, The global biogeography of semi-arid periodic vegetation patterns, *Global Ecol. Biogeogr.* 17 (2008), 715–723.

[4] L. Desiderio, S. Falletta, M. Ferrari and L. Scuderi, CVEM-BEM, coupling for the simulation of time-domain wave fields scattered by obstacles with complex geometries, *Comput. Methods Appl. Math.* 23 (2023), 353–372.

[5] K. Diethelm, *The Analysis of Fractional Differential Equations*, Springer-Verlag, Berlin, 2004.

[6] A. Doelman, R.A. Gardner and T.J. Kaper, Stability analysis of singular patterns in the 1d Gray-Scott model: a matched asymptotics approach, *Phys. D* 122 (1998), 1–36.

[7] V. Gafiychuk and B. Datsko, Pattern formation in a fractional reaction-diffusion system, *Phys. Rev. A Stat. Mech. Appl.* 365 (2006),300-306.

[8] P. Gray and S.K. Scott, Autocatalytic reactions in the isothermal continuous stirred tank reactor: isolates and other forms of multistability, *Chem. Eng. Sci.* 38 (1983), 29-43.

[9] A. Jannelli, M. Ruggieri, M.P. Speciale; Numerical solutions of space-fractional advection-diffusion equation with a source term, *AIP Conf. Proc.* (2019); 2116 (1): 280007.

[10] A. Jannelli and M.P. Speciale, On the numerical solutions of coupled nonlinear time-fractional reaction-diffusion equations, *AIMS Math.* 6 (2021), 9109-9125.

[11] A. Jannelli, Numerical solutions of fractional differential equations arising in engineering sciences, *Mathematics* 8 (2020), 215.

[12] A. Jannelli and M.P. Speciale, Exact and numerical solutions of two-dimensional time-fractional diffusion–reaction equations through the Lie symmetries, *Nonlinear Dyn.* 105 (2021), 2375-2385.

[13] A. Jannelli and M.P. Speciale, On the Solutions of the Fractional Generalized Gierer-Meinhardt Model, *Fractional Differential Equations: Modeling, Discretization, and Numerical Solvers*, 50, 91-105, Springer Nature Singapore, 2023.

[14] A. Jannelli and M.P. Speciale, Fractional boundary layer flow: Lie symmetry analysis and numerical solution, *Mathematics* 12 (2024), 184.

[15] A. Jannelli and M.P. Speciale, Fractional Vegetation-Water Model in Arid and Semi-Arid Environments: Pattern Formation and Numerical Simulations. Submitted to Mathematics and Computers in Simulation. Available at arXiv:2510.19827, 2025.

[16] C.A. Klausmeier, Regular and irregular patterns in semiarid vegetation, *Sci.* 284 (1999), 1826-1828.

[17] W.A. Macfadyan, Soil and vegetation in British Somaliland, *Nat.* 165 (1950), 121.

[18] W.A. Macfadyan, Vegetation patterns in the semi-desert planes of British Somaliland, *Geogr. J.* 116 (1950), 199–211.

[19] F. Oliveri and M.P. Speciale, Reduction of balance laws to conservation laws by means of equivalence transformations, *J. Math. Phys.* 54 (2013), 041506.

[20] I. Podlubny, Fractional Differential Equations: An Introduction to Fractional Derivatives, Fractional Differential Equations, Some Methods of Their Solution and Some of Their Applications, Academic Press, San Diego, 1999.

[21] A.S.V. Ravi Kanth, K. Aruna and K. Raghavendar, Natural transform decomposition method for the numerical treatment of the time fractional Burgers–Huxley equation, *Numer. Methods Partial Differ. Equations* 39 (2023), 2690–2718.

[22] M. Rietkerk, O. Ketner, J. Burger, B. Hoorens and H. Olff, Multiscale soil and vegetation patchiness along a gradient of herbivore impact in a semi-arid grazing system in West Africa, *Plant. Ecolog.* 148 (2000), 207–224.

[23] M. Rietkerk, S.C. Dekker, P.C. de Ruiter and J. van de Koppel, Self-organized patchiness and catastrophic shifts in ecosystems, *Sci.* 305 (2004), 1926–1929.

[24] J.A. Sherratt, An analysis of vegetation stripe formation in semi-arid landscapes, *J. Math. Biol.* 51 (2005), 183-197.

[25] J.A. Sherratt and G.J. Lord, Nonlinear dynamics and pattern bifurcations in a model for vegetation stripes in semi-arid environments, *Theor. Popul. Biol.* 71 (2007), 1-11.

[26] J.A. Sherratt, Pattern solutions of the Klausmeier model for banded vegetation in semi-arid environments I, *Nonlinearity* 23 (2010), 2657-2675.

[27] J.A. Sherratt, Pattern solutions of the Klausmeier model for banded vegetation in semi–arid environments II: patterns with the largest possible propagation speeds, *Proc. R. Soc. A* 467 (2011), 3272-3294.

[28] C. Valentin, J.M. d'Herbes and J. Poesen, Soil and water components of patterns, *Catena* 37 (1999), 1-24

[29] S. van der Stelt, A. Doelman, G. Hek et al., Rise and fall of periodic patterns for a generalized Klausmeier–Gray–Scott model, *J. Nonlinear Sci.* 23 (2013), 39–95.